CHINESE OPTICS LETTERS

Vol. 19, No. 8 | August 2021

Ultra-low detection delay drift caused by the temperature variation in a Si-avalanche-photodiode-based single-photon detector

Yurong Wang (王煜蓉), Linli Wang (汪琳莉), Chenyi Wu (吴琛怡), Zhaohui Li (李召辉)*, Lei Yang (杨 雷), and Guang Wu (吴 光)**

State Key Laboratory of Precision Spectroscopy, East China Normal University, Shanghai 200241, China

*Corresponding author: zhhli@lps.ecnu.edu.cn

**Corresponding author: gwu@phy.ecnu.edu.cn

Received October 1, 2020 | Accepted December 21, 2020 | Posted Online April 13, 2021

We report a method to reduce the detection delay temperature drift for a single-photon detector based on the avalanche photodiode (SPAD). Both the SPAD and the comparator were temperature stabilized, resulting in an ultra-low temperature drift at 0.01 ps/°C. A stable time deviation as 0.15 ps over 1000 s was realized, while the ambient temperature fluctuated rapidly from 24°C to 44°C. To the best of our knowledge, this is the first report on the ultra-stable delay SPAD detector in the case of rapid increase or decrease of ambient temperature. It is helpful to improve the stability of onboard detectors for optical laser time transfer between ground and space.

Keywords: avalanche photodiodes; laser ranging; single-photon detection; stability; temperature dependence.
DOI: 10.3788/COL202119.082502

1. Introduction

In recent years, time of flight (TOF) laser ranging by single-photon detection has been widely used in satellite laser ranging, orbiting space debris detection, laser time transfer, laser communications, and so on[1–5]. TOF measurement is based on the time correlation between the synchronization pulses and the receiving photons to obtain accurate distance information of the targets[6]. In order to realize a high precision and ultra-stable measurement, the single-photon detector with low timing jitter and high stability is significantly demanded, especially for the laser time transfer applications, where the accuracy and stability of the entire chain have been reached at tens of picoseconds (ps) and sub-ps, respectively[7]. The current goal of the global geodetic observing system (GGOS) to achieve 1 mm accuracy and 0.1 mm/year stability presents the largest challenge to the photon counting laser ranging system[8]. The project of European Laser Timing (ELT) under construction has set the ultimate stability of the entire single-photon laser ranging chain expressed by the time deviation (TDEV) to be 0.3 ps over 300 s[9,10].

By now, different kinds of single-photon detectors have been implemented in the laser ranging systems. Photomultiplier tube detectors (PMTs) with large active area are favorable for collecting the weak returning photon stream[11], whereas its timing jitter is typically on the order of hundreds of ps to a few nanoseconds[12]. Although the micro-channel plate PMT with a timing jitter of about 40 ps is developed[13], the high operation voltage and susceptibility to the external magnetic field effect will limit its scalability, especially for applications in space. Recent progress in the superconducting nanowire single-photon detector makes high-efficiency and low-noise detection of photons at eye-safe wavelengths possible[14,15], especially since its timing jitter has been reduced to 14.8 ps[16]. But, efficiently coupling the echo photons to the fiber pigtail of the superconducting nanowire single-photon detector is still a challenge in the laser ranging system. Besides, the cryogenic operation temperature makes it hard to be used in environments other than ground base stations. Single-photon detectors based on avalanche photodiodes (PDs) have gained a lot of visibility, especially in the laser time transfer application, due to their small size, large operation temperature range, and ps timing response compatible with high-precision time-resolved sensing systems[17–19]. However, the performance of this kind of detector is greatly influenced by temperature[20,21], which will impact the measurement accuracy and stability.

The single-photon avalanche PD (SPAD) usually operates in Geiger mode, in which a reverse bias voltage higher than the breakdown voltage is supplied. However, when the operation temperature increases, the breakdown voltage of the SPAD chip will increase, leading to the change of the avalanche gain, and

hence influence the detection efficiency, dark count, timing jitter, and other important parameters[22]. Moreover, in the SPAD detector module, ultrafast comparator (CO) chips are usually used as one of the key components to extract and convert the avalanche pulses into the digital output. However, its inherent propagation delay will also vary with the temperature, resulting in a large detection delay fluctuation. Even if a CO chip with extremely low temperature drift is implemented, a delay drift of hundreds of femtoseconds per °C would be introduced, causing the instability of the single-photon detector[23]. The Changchun laser ranging station decreases the temperature drift by shielding the detector in a relatively stable temperature environment[20]. A temperature controller for the SPAD chip is a common solution to reduce the temperature influence, but it cannot completely prevent the drift caused by the CO[24]. Recently, the research group at Czech Technical University proposed to use a signal coaxial cable with a specific length that has a negative propagation delay dependent on the temperature for the detector to compensate the detector temperature drift to 6 fs/°C, and 40 fs over 10,000 s TDEV for the entire time-correlated single-photon counting (TCSPC) measurement chain was realized, while the ambient temperature is constant[25].

Here, we propose an approach to decrease the temperature drift effect on the detection delay of the Si-SPAD and demonstrate an extremely low temperature drift coefficient of 0.01 ps/°C despite the ambient temperature variation by stabilizing the temperature of the key components in the detector module. With this method, the detection delay was no longer sensitive to the ambient temperature, providing a long-term detection delay stability characterized by TDEV as low as 0.15 ps for an averaging time of 1000 s, even when the ambient temperature fluctuated rapidly from 24°C to 44°C. Such a detector can be used in space with complex temperature variations, as well as in an outdoor laser ranging system, especially for the application of laser time transfer.

2. Experiments and Results

The Si-SPAD used in the experiment here had an active area of 200 μm in diameter and a breakdown voltage of 33 V at 10°C, developed by Beijing University of Posts and Telecommunications[26]. It was operated in Geiger mode and connected with an active quenching and gating circuit to complete the avalanche detection and suppression, as shown in Fig. 1. The SPAD chip was mounted into a transistor outline (TO-8) package vacuum cell equipped with a three-stage thermoelectric cooler, which was controlled by a proportional–integral–derivative (PID) temperature control module (TCM 1) set to 10°C within ±0.5°C. The corresponding thermistor sensor (Sensor 1) was attached to the surface of the SPAD chip, and a PID TCM 2 was installed for the CO chip with a corresponding thermistor sensor (Sensor 2) on its surface preset to 15°C within ±0.5°C. In this detector, the temperature of the CO was 5°C higher than that of the other electronic components on the circuit board when the detector was operating without any

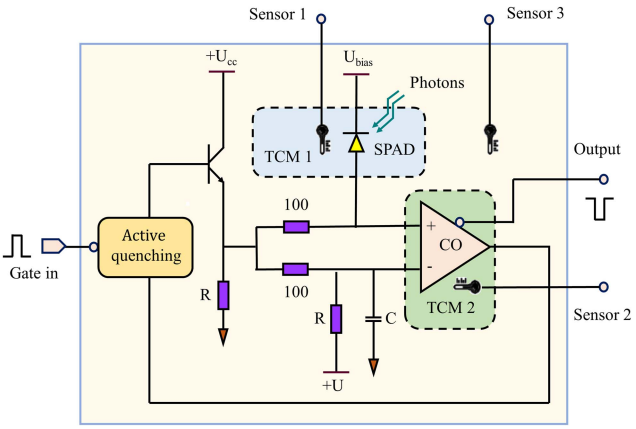

Fig. 1. Simplified circuit for the SPAD detector with temperature controlling. SPAD, single-photon avalanche photodiode; CO, the ultrafast comparator; TCM 1, 2, temperature control module of the SPAD chip and of the CO chip, respectively.

temperature controller. In order to get a larger constant operation temperature range, the CO's presetting temperature was also 5°C higher than that of the SPAD chip. The whole detector module was integrated in an aluminum housing of 110 mm × 65 mm × 35 mm. A third thermistor sensor (Sensor 3) was installed in the detector housing to monitor the temperature change of the whole module. An external thermoelectrical board TCM 3 was used to change the ambient temperature for the test. In this experiment, the bias voltage of the SPAD was fixed at 2.3 V above its breakdown voltage, providing a detection efficiency of 50% at 532 nm and a dark count rate of 110 kHz. Considering the high background photon flux in the intended space and outdoor applications, the inherent dark count rate could be acceptable[21]. The timing resolution of the SPAD module was measured to be 44 ps (full width at half-maximum, FWHM).

We established a TCSPC experiment to measure the temporal profiles of the SPAD module, as shown in Fig. 2. A 532 nm pulsed laser with 28 ps pulse width was employed as the light

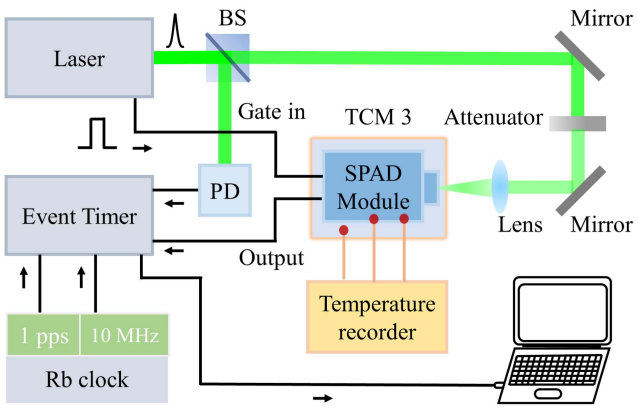

Fig. 2. Simplified scheme of the TCSPC chain. BS, beam splitter; PD, photodiode; Rb clock, rubidium reference clock; TCM 3, temperature control module for the detector.

source. The repetition rate was 10 kHz. After attenuating to about 0.2 photon/pulse, the light was focused onto the SPAD chip by a convex lens with a beam spot smaller than the active area of the SPAD chip to ensure all the photons to impinge on the detector. A PD was used to provide a synchronous signal for the event timer, which was used to record the interval time between the emission of the laser pulse and the reception of the photon signal. An external 1 pps reference signal and a 10 MHz frequency source from a rubidium clock were sent into the event timer to set up the time scales, providing a ps timing resolution and femtosecond timing stability. Figure 3 shows the experimental setup and SPAD package. The overall timing resolution of the system was about 56 ps (FWHM) according to

$$F = \sqrt{\Delta_l^2 + \Delta_t^2 + \Delta_d^2}, \tag{1}$$

where Δ_l is the width of the laser pulse of 28 ps, Δ_t is the jitter of the timing system of 21 ps, and Δ_d is the jitter of the detector itself of 44 ps.

As we heated the SPAD module by TCM 3, the temperature of each sensor was recorded by the multi-channel temperature recorder in real time. At first, only TCM 1 was operated to make sure that the SPAD chip could operate at a constant temperature, while TCM 2 was disconnected so that the temperature of the CO chip varied with the ambient temperature, similar to the other electronic components. We measured the temperature drift of the detector by the TCSPC setup at different temperatures recorded by Sensor 3 and found out that the detection delay had shifted more than 10 ps when the temperature varied within 18–45°C, as shown in Fig. 4(a). The detection delay increased linearly with the increasing temperature of the SPAD module with a slope of 0.38 ps/°C, as shown in Fig. 4(b).

In order to investigate the contribution of the CO chip in the module to the temperature drift, we measured its electrical signal propagation delay as a function of temperature separately. A transistor–transistor logic (TTL) signal from an analog function generator was divided into two channels. One was fed to the CO chip as the electrical input, and the other one was sent to the event timer as a trigger signal, whereby the propagation delay between the TTL and the output of the CO chip could be measured by the event timer. As TCM 3 heated the module, the temperature of the CO chip changed accordingly. The propagation delay shifted about 9.66 ps as the temperature increased from 18°C to 45°C, providing a linear dependence of the detection delay on the temperature with a slope of 0.36 ps/°C, as shown in Figs. 4(c) and 4(d). Therefore, we can conclude that given that the SPAD chip temperature is stabilized, and the temperature delay drift is mainly from the signal propagation delay of the CO chip.

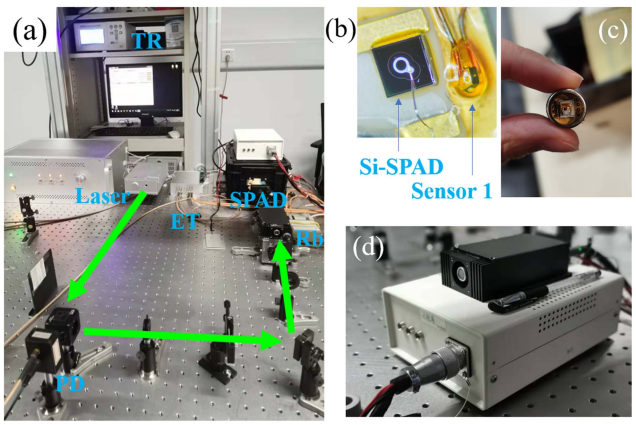

Fig. 3. (a) Experimental setup. TR, temperature recorder; ET, event timer. (b) Si-SPAD chip. (c) SPAD chip with three-stage thermoelectric cooler in TO-8 housing. (d) SPAD detector module.

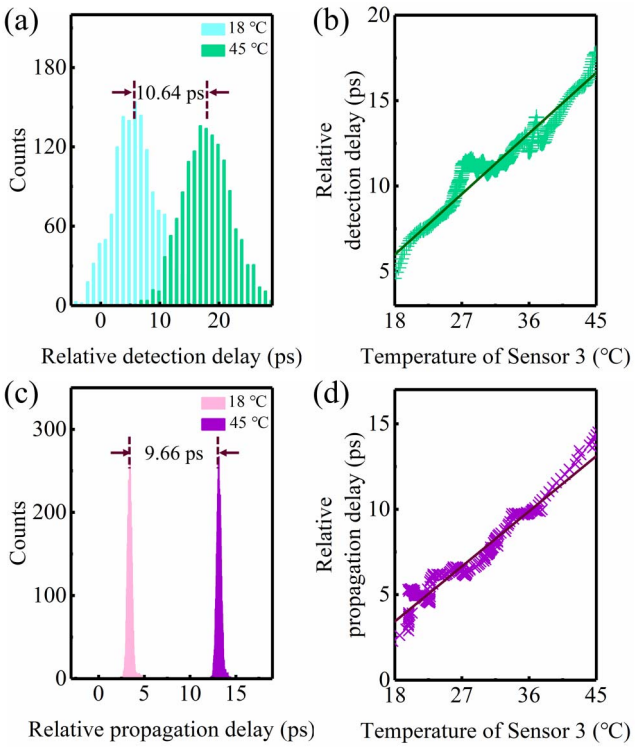

Fig. 4. (a) Detection delay of the detector at 18°C and 45°C, respectively. (b) Linear dependence of the detection delay of the SPAD module on its temperature. (c) Propagation delay of the CO chip at 18°C and 45°C, respectively. (d) Relative propagation delay as a function of the CO's temperature.

So, we packed the CO chip in a vacuum cell like the SPAD chip and used TCM 2 to stabilize the temperature of the CO chip at 15°C within ±0.5°C. We monitored the detection delay of the SPAD module as TCM 3 changed the temperature; meanwhile, the temperatures of the SPAD chip, the CO chip, and the whole module were recorded by Sensor 1 to Sensor 3, respectively, as shown in Fig. 5(a). The detection delay of the entire SPAD module was stabilized with a standard deviation of 0.27 ps during the whole test of 120 min when the ambient temperature changes from 24°C to 44°C several times, as shown in Fig. 5(b). It is worth mentioning that since this method was a passive control of the detection delay, it would not change the working condition of the detector itself. Therefore, the key characters of the SPAD module, such as timing resolution, detection efficiency, and dark count rate, would be maintained. However, when affected by the

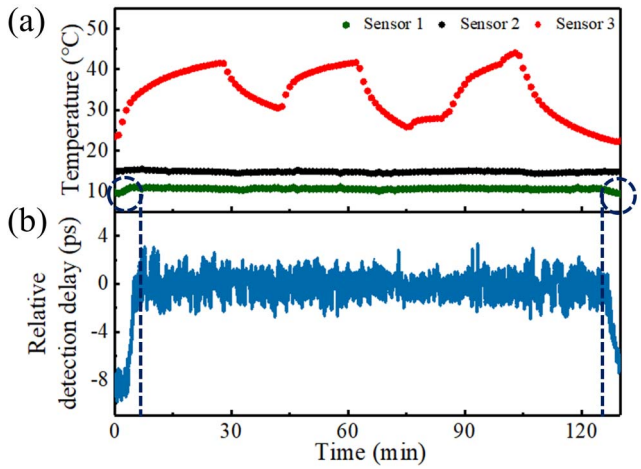

Fig. 5. (a) Real-time temperature monitored by Sensors 1–3 during the test of about 120 min. (b) Stabilized real-time relative detection delay.

heat dissipation for TCM 1 in such an integrated SPAD module, the stabilized operating temperature of the SPAD chip was between 24°C and 44°C. At the beginning and also at the end of the test, the relative detection delay drifted due to the out of control of TCM 1 when the ambient temperature was below 24°C or above 44°C, as shown in Fig. 5(b). The stabilized operation temperature range could be enlarged by a better design of dissipation.

Then, we extracted the relative detection delay as a function of the ambient temperature according to Fig. 5 to demonstrate the linear dependence of the detection delay on the temperature, as shown in Fig. 6(a). Each point was the average of 24 experimental data of the detection delay measured at the same temperature during the test of 120 min, and the error bars were obtained by the standard deviation of the experimental data at the same temperature. The linear fit of the data shows that a slope of 0.01 ps/°C was achieved. Compared to the temperature drift

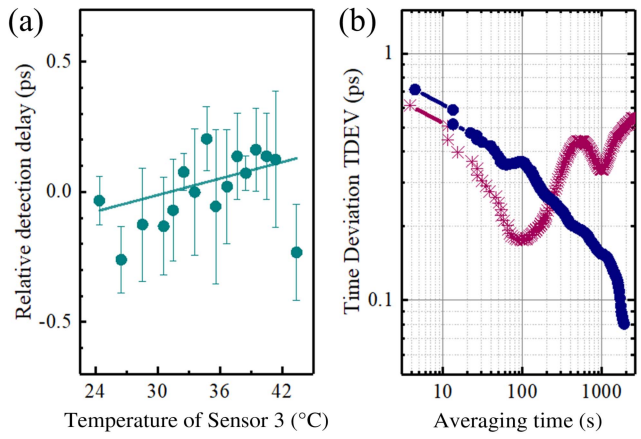

Fig. 6. (a) Relative detection delay dependent on the ambient temperature. Solid line is the linear fit of the experiment data. (b) The TDEV before and after optimization within a temperature variation of 24°C to 44°C.

without the temperature stabilization on the CO chip in Fig. 4(b), the slope of the curve decreased dramatically, indicating that this method has a significant effect on reducing the single-photon detector's temperature drift. Owing to the small detection delay drift within a temperature variation of 20°C, 0.15 ps over an averaging time of 1000 s TDEV has been reached for the entire TCSPC chain, as shown by the blue line in Fig. 6(b). The purple line in Fig. 6(b) is the TDEV result before optimization. The long-term TDEV was remarkably improved through decreasing the detector's temperature drift by stabilizing the temperature of both the SPAD and the CO chips. To the best of our knowledge, this is the first report on an ultra-stable delay SPAD detector in case of rapid increase or decrease of ambient temperature. It is suitable especially for applications in space environments where the temperature changes are unpredictable.

In principle, the method described above could be implemented in different kinds of single-photon detectors with temperature-sensitive components for applications with high requirements on detection delay stability in complex temperature variation environments, such as outdoor laser ranging systems and optical laser time transfer. Besides the SPAD chip and the CO chip, there are other temperature-sensitive components in the SPAD module, such as the switching transistor and the resistors. Better detection delay stability would be achieved if lower temperature drift coefficient resistors and transistors are implemented when the operation temperature of SPAD and CO chips was fixed well.

3. Conclusion

In this work, we improved the detection delay stability in temperature variation environments by reducing the detection delay temperature dependence of the single-photon detector based on SPAD. We packed both the SPAD chip and the ultrafast CO in separate vacuum TO-8 packages and applied temperature control on them individually to ensure that these two core chips operate stably in the detector. The detection delay standard deviation of the whole SPAD module was 0.27 ps over 2 h of operation when the ambient temperature changed from 24°C to 44°C. Within the temperature variation range, a 0.01 ps/°C detection delay temperature drift of the detector and a 0.15 ps over 1000 s timing stability of the entire TCSPC chain represented by TDEV were achieved, enabling the detector to be used in outdoor applications with complex temperature variations, such as satellite laser ranging and optical laser time transfer.

Acknowledgement

This work was supported by the National Key R&D Program of China (No. 2016YFB0400904), National Natural Science Foundation of China (Nos. 11774095, 11804099, and 11621404), Shanghai Basic Research Project (No. 18JC1412200), and Program of Introducing Talents of Discipline to Universities (No. B12024).

References

1. Y. Yu, B. Liu, and Z. Chen, "Analyzing the performance of pseudo-random single photon counting ranging lidar," Appl. Opt. **57**, 7733 (2018).
2. F. Villa, B. Markovic, S. Bellisai, D. Bronzi, A. Tosi, F. Zappa, S. Tisa, D. Durini, S. Weyers, U. Paschen, and W. Brockherde, "SPAD smart pixel for time-of-flight and time-correlated single-photon counting measurements," IEEE Photon. J. **4**, 795 (2012).
3. H. Zhang, M. Long, H. Deng, Z. Wu, Z. Cheng, and Z. Zhang, "Space debris laser ranging with a 60 W single-frequency slab nanosecond green laser at 200 Hz," Chin. Opt. Lett. **17**, 051404 (2019).
4. H. P. Plag and M. R. Pearlman, *Global Geodetic Observing System* (Springer, 2009).
5. D. Yang, Y. Huang, T. Liu, X. Ma, X. Duan, K. Liu, and X. Ren, "Bias-free operational monolithic symmetric-connected photodiode array," Chin. Opt. Lett. **18**, 012501 (2020).
6. Y. Liang, J. Huang, M. Ren, B. Feng, X. Chen, E. Wu, G. Wu, and H. Zeng, "1550-nm time-of-flight ranging system employing laser with multiple repetition rates for reducing the range ambiguity," Opt. Express **22**, 4662 (2014).
7. I. Prochazka, J. Kodet, J. Blazej, G. Kirchner, F. Koidl, and P. Wang, "Identification and calibration of one-way delays in satellite laser ranging systems," Adv. Space Res. **59**, 2466 (2017).
8. M. Wilkinson, U. Schreiber, I. Procházka, C. Moore, J. Degnan, G. Kirchner, Z. Zhongping, P. Dunn, V. Shargorodskiy, M. Sadovnikov, C. Courde, and H. Kunimori, "The next generation of satellite laser ranging systems," J. Geodesy **93**, 2227 (2019).
9. M. P. Heß, L. Stringhetti, B. Hummelsberger, K. Hausner, R. Stalford, R. Nasca, L. Cacciapuoti, R. Much, S. Feltham, T. Vudali, B. Léger, F. Picard, D. Massonnet, P. Rochat, D. Goujon, W. Schäfer, P. Laurent, P. Lemonde, A. Clairon, P. Wolf, C. Salomon, I. Procházka, U. Schreiber, and O. Montenbruck, "The ACES mission: system development and test status," Acta Astronaut. **69**, 929 (2011).
10. U. Schreiber, I. Prochazka, P. Lauber, U. Hugentobler, W. Schafer, L. Cacciapuoti, and R. Nasca, "The European Laser Timing (ELT) experiment on-board ACES," in *Proceedings of IEEE – International Frequency Control Symposium* (2009), p. 594.
11. S. Donati and T. Tambosso, "Single-photon detectors: from traditional PMT to solid-state SPAD-based technology," IEEE J. Quantum Electron. **20**, 204 (2014).
12. F. Acerbi, A. Ferri, A. Gola, M. Cazzanelli, L. Pavesi, N. Zorzi, and C. Piemonte, "Characterization of single-photon time resolution: from single SPAD to silicon photomultiplier," IEEE T. Nucl. Sci. **61**, 2678 (2014).
13. K. Inami, "MCP-PMT production for Belle II TOP detector and further R&D," Nucl. Instrum. Meth. A **936**, 556 (2018).
14. A. Divochiy, M. Misiaszek, Y. Vakhtomin, P. Morozov, K. Smirnov, P. Zolotov, and P. Kolenderski, "Single photon detection system for visible and infrared spectrum range," Opt. Lett. **43**, 6085 (2018).
15. L. Xue, M. Li, L. Zhang, D. Zhai, Z. Li, L. Kang, Y. Li, H. Fu, M. Ming, S. Zhang, X. Tao, Y. Xiong, and P. Wu, "Long-range laser ranging using superconducting nanowire single-photon detectors," Chin. Opt. Lett. **14**, 071201 (2016).
16. L. You, J. Quan, Y. Wang, Y. Ma, X. Yang, Y. Liu, H. Li, J. Li, J. Wang, J. Liang, Z. Wang, and X. Xie, "Superconducting nanowire single photon detection system for space applications," Opt. Express **26**, 2965 (2018).
17. J. M. Pavia, M. Wolf, and E. Charbon, "Single-photon avalanche diode imagers applied to near-infrared imaging," IEEE J. Quantum Electron. **20**, 291 (2014).
18. B. Du, C. Pang, D. Wu, Z. Li, H. Peng, Y. Tao, E Wu, and G. Wu, "High-speed photon-counting laser ranging for broad range of distances," Sci. Rep. **8**, 1 (2018).
19. Z. Li, E. Wu, C. Pang, B. Du, Y. Tao, H. Peng, H. Zeng, and G. Wu, "Multi-beam single-photon-counting three-dimensional imaging lidar," Opt. Express **25**, 10189 (2017).
20. X. Dong, X. W. Han, C. B. Fan, and Q. L. Song, "Improvements of Changchun SLR station," in *Proceedings of the 20th International Laser Ranging Workshop* (2016), p. 1.
21. K. U. Schreiber, I. Prochazka, P. Lauber, U. Hugentobler, W. Schäfer, L. Cacciapuoti, and R. Nasca, "Ground-based demonstration of the European Laser Timing (ELT) experiment," IEEE Trans. Ultrason. Free. **57**, 728 (2010).
22. M. Hofbauer, B. Steindl, and H. Zimmermann, "Temperature dependence of dark count rate and after pulsing of a single-photon avalanche diode with an integrated active quenching circuit in 0.35 μm CMOS," J. Sens. **2018**, 9585931 (2018).
23. I. Prochazka, J. Kodet, J. Eckl, and J. Blazej, "Note: large active area solid state photon counter with 20 ps timing resolution and 60 fs detection delay stability," Rev. Sci. Instrum. **88**, 106105 (2017).
24. I. Prochazka, J. Kodet, and J. Blazej, "Note: solid state photon counters with sub-picosecond timing stability," Rev. Sci. Instrum. **84**, 046107 (2013).
25. I. Prochazka, J. Blazej, T. Flekova, and J. Kodet, "Silicon based photon counting detector providing femtosecond detection delay stability," IEEE J. Quantum Electron. **26**, 3900205 (2020).
26. H.-Y. Zhang, L.-L. Wang, C.-Y. Wu, Y.-R. Wang, L. Yang, H.-F. Pan, Q.-L. Liu, X. Guo, K. Tang, Z.-P. Zhang, and G. Wu, "Avalanche photodiode single-photon detector with high time stability," Acta Phys. Sin. **69**, 074204 (2020).